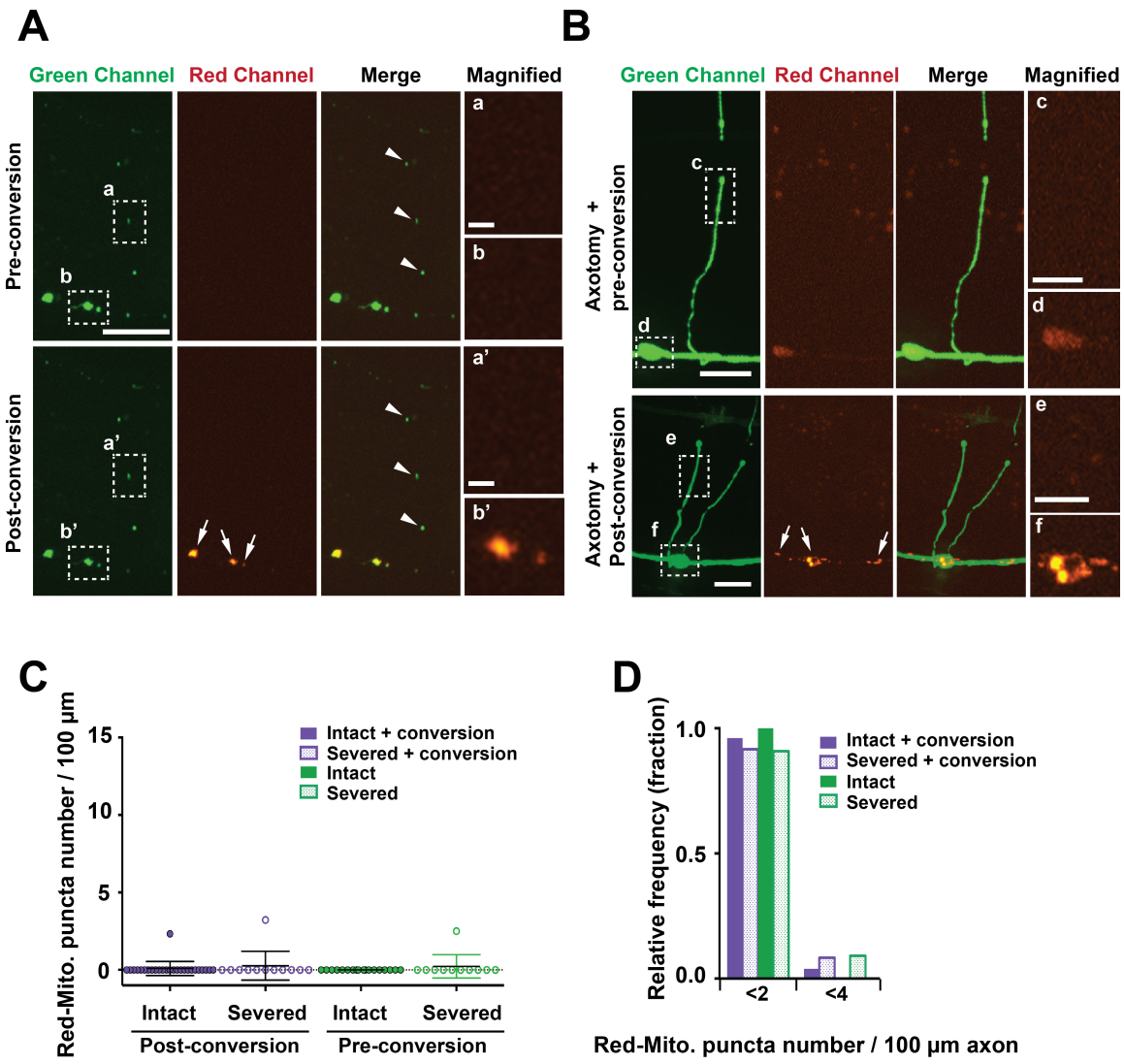

Figure S1. Related to Figure 2. Selective photoconversion specifically changes the color of mito-Dendra2 only in the VNC.

(A) Mito::Dendra2 in GABA axons before (upper) or immediately after (bottom) photoconversion using 405 nm laser. Arrowheads indicate a single Mito::Dendra2 signal within axon. Arrows indicate photoconverted red-Mito::Dendra2 on VNC. Boxes are magnified in the right panels. Scale bars are 20 µm.

(B) Mito::Dendra2 in the axotomized GABA axons before (upper) or immediately after (bottom) photoconversion using 405 nm laser. Axotomy did not convert the fluorescent color of Mito::Dendra2 in axons. Arrows indicate photoconverted red-Mito::Dendra2 on VNC. Boxes are magnified in the right panels. Scale bars are 10 µm.

(C and D) Scatter plot (C) and binned frequency graph (D) showing mitochondria density in GABA axons in given conditions. (C) Dots indicate individual axon's mitochondrial density. Error bars indicate 95% confidence interval. Statistical significance was calculated by the Mann–Whitney test.

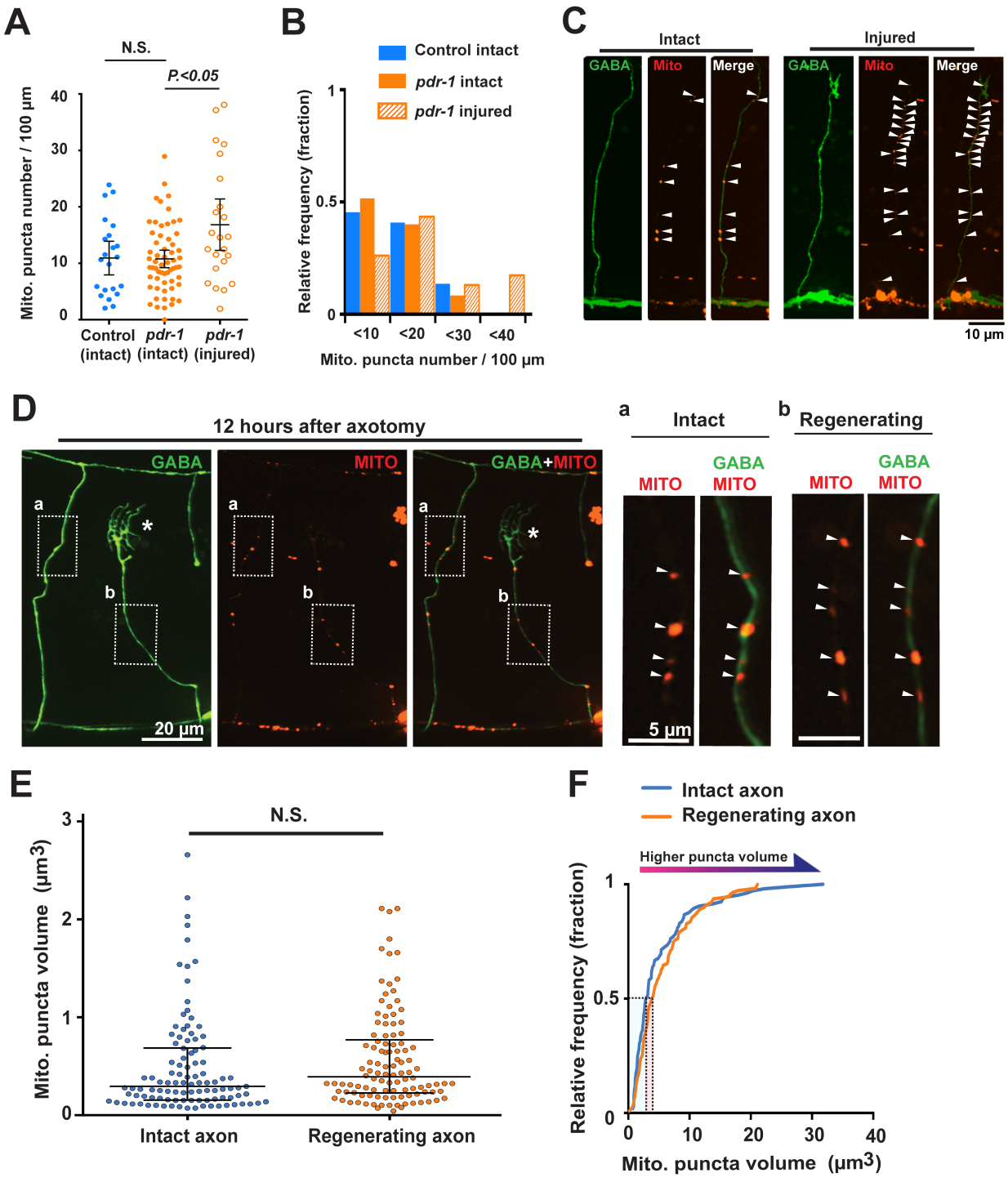
A
N.S.
P.<0.05
Mito. puncta number / 100 µm
40
30
20
10
0
Control (intact)
pdr-1 (intact)
pdr-1 (injured)
B
Control intact
pdr-1 intact
pdr-1 injured
Relative frequency (fraction)
1
0.5
0
<10
<20
<30
<40
Mito. puncta number / 100 µm
C
Intact
Injured
GABA
Mito
Merge
10 µm
D
12 hours after axotomy
GABA
MITO
GABA+MITO
a
b
20 µm
a Intact
b Regenerating
MITO
GABA MITO
5 µm
E
N.S.
Mito. puncta volume (µm3)
3
2
1
0
Intact axon
Regenerating axon
F
Intact axon
Regenerating axon
Higher puncta volume
Relative frequency (fraction)
1
0.5
0
0
10
20
30
40
Mito. puncta volume (µm3)

Figure S2. Related to Figure 2. **Defective mitophagy and increased mitochondrial fission are not main cause of the mitochondrial density increase within axons after injury.**

(A and B) Scatter plot (A) and binned frequency graph (B) showing mitochondria density in GABA axons of *pdr-1* mutants with or without injury. (A) Bars indicate average ± 95% confidence interval. Statistical significance was calculated by the Mann–Whitney test.

(C) Increased Mito::mCherry puncta in axons of *pdr-1* mutants after injury. Arrowheads indicate individual mito::mCherry puncta.

(D) Mitochondria in GABA axons 24 hours after injury. Arrowheads indicate a single Mito::mCherry signal. Asterisks indicate the tips of regenerating axons.

(E) Scatter plot showing mitochondria volume in GABA axons after injury compared to intact axons. Dots indicate individual mitochondria volumes. Lines indicate median and error bars indicate 95% confidence interval. Statistical significance was calculated by the Mann–Whitney test.

(F) Cumulative frequency histogram of mitochondria volumes.

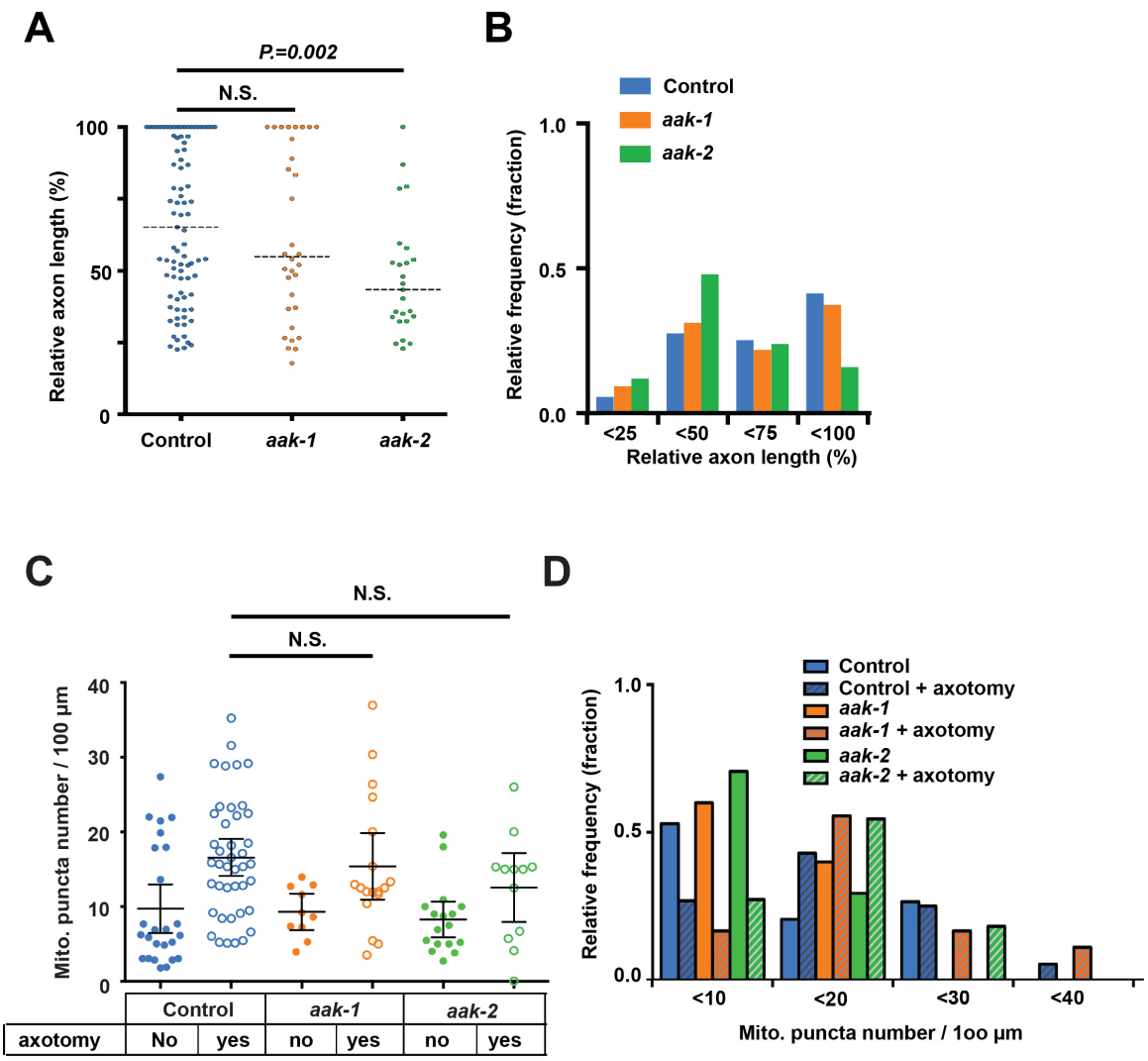

Figure S3. Related to Figure 2. AMPK mutants have normal mitochondrial density in axons.

(A and B) Scatter plot (A) and binned frequency graph (B) showing relative axon length of given animals 24 hours after axotomy. (A) Dashed lines indicate median. Statistical significance was calculated by the Mann–Whitney test.

(C and D) Scatter plot (C) and binned frequency graph (D) showing mitochondria density in GABA axons of *aak-1* and *aak-2* mutants with or without injury. (C) Bars indicate average ± 95% confidence interval. Statistical significance was calculated by the Mann–Whitney test.

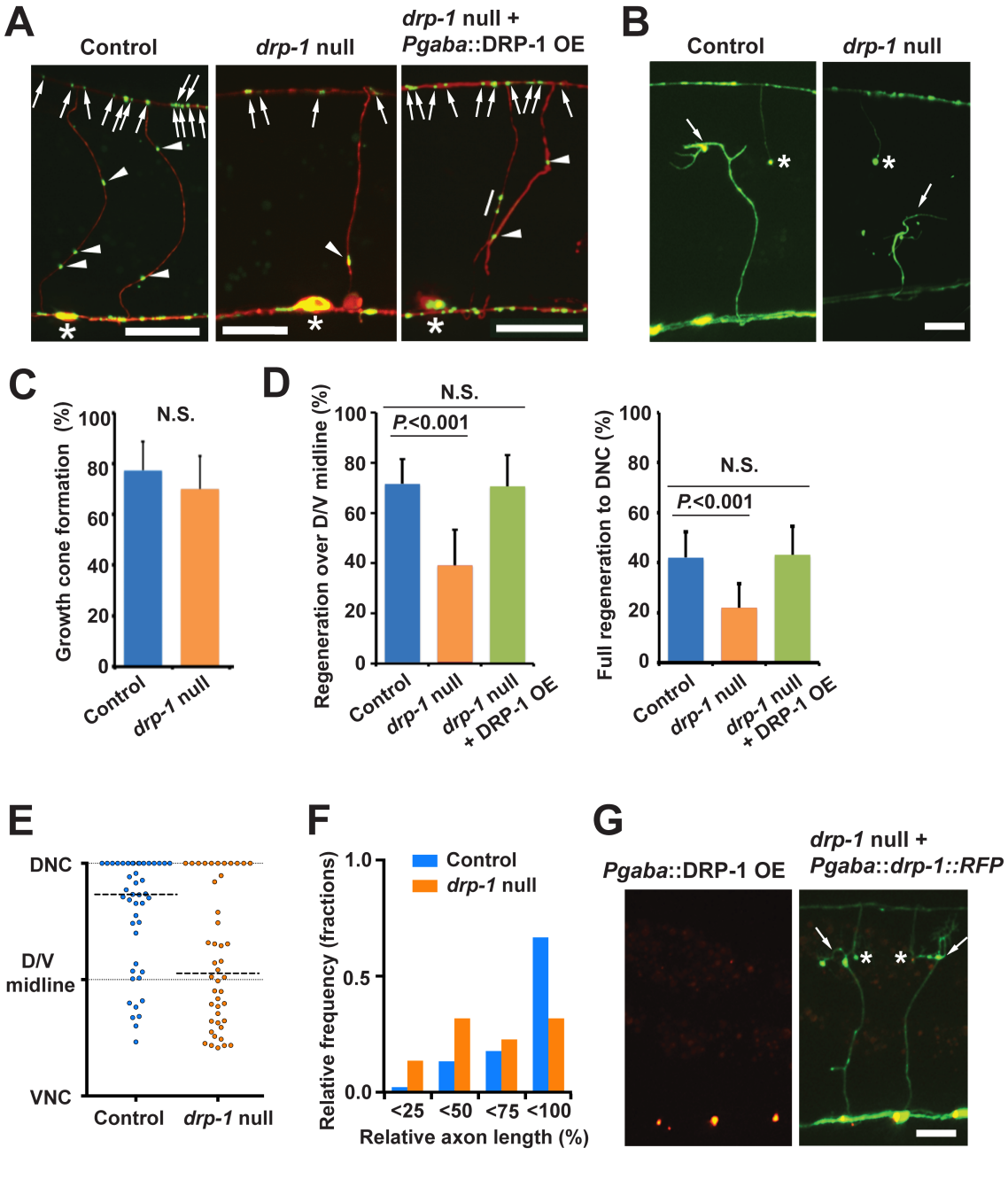
A
Control
drp-1 null
drp-1 null +
Pgaba::DRP-1 OE
B
Control
drp-1 null
C
Growth cone formation (%)
N.S.
Control
drp-1 null
D
Regeneration over D/V midline (%)
N.S.
P.<0.001
Control
drp-1 null
drp-1 null
+ DRP-1 OE
Full regeneration to DNC (%)
N.S.
P.<0.001
Control
drp-1 null
drp-1 null
+ DRP-1 OE
E
DNC
D/V
midline
VNC
Control
drp-1 null
F
Relative frequency (fractions)
Control
drp-1 null
<25
<50
<75
<100
Relative axon length (%)
G
Pgaba::DRP-1 OE
drp-1 null +
Pgaba::drp-1::RFP

Figure S4. Related to Figure 4. DRP-1 loss decreases mitochondria density and axon regeneration.

(A) Abnormal mitochondrial division and distribution in GABA axons of *drp-1* null mutants. Scale bars are 20 μm. Arrowheads indicate individual mCherry puncta in commissures; arrows indicate individual mCherry puncta in nerve cords.

(B) GABA axons 24 hours after axotomy in control animals and *drp-1* null mutant. Scale bars are 20 μm.

(C) Growth cone formation 24 hours after axotomy. Error bars indicate 95% confidence interval. Statistical significance was calculated by Fisher's exact test. N is 81 (control) and 41 *(drp-1* null).

(D) Regeneration over dorsal-ventral midline (left) or full regeneration to the dorsal nerve cord (right) 24 hours after axotomy. Error bars indicate 95% confidence interval. Statistical significance was calculated by Fisher's exact test. N is 81 (control), 41 *(drp-1* null) and 51 (*drp-1* null + DRP-1 OE).

(E and F) Scatter plot (E) and binned frequency graph (F) of relative axon length of GABA axons 24 hours after axotomy. Dots indicate individual axons and lines indicate median. Horizontal dashed lines indicate median. Statistical significance was calculated by Mann–Whitney test.

(G) GABA axons 24 hours after axotomy in *drp-1* mutant expressing *drp-1::RFP* under the *unc-47* GABAergic neuronal promoter. Scale bars are 20 μm.

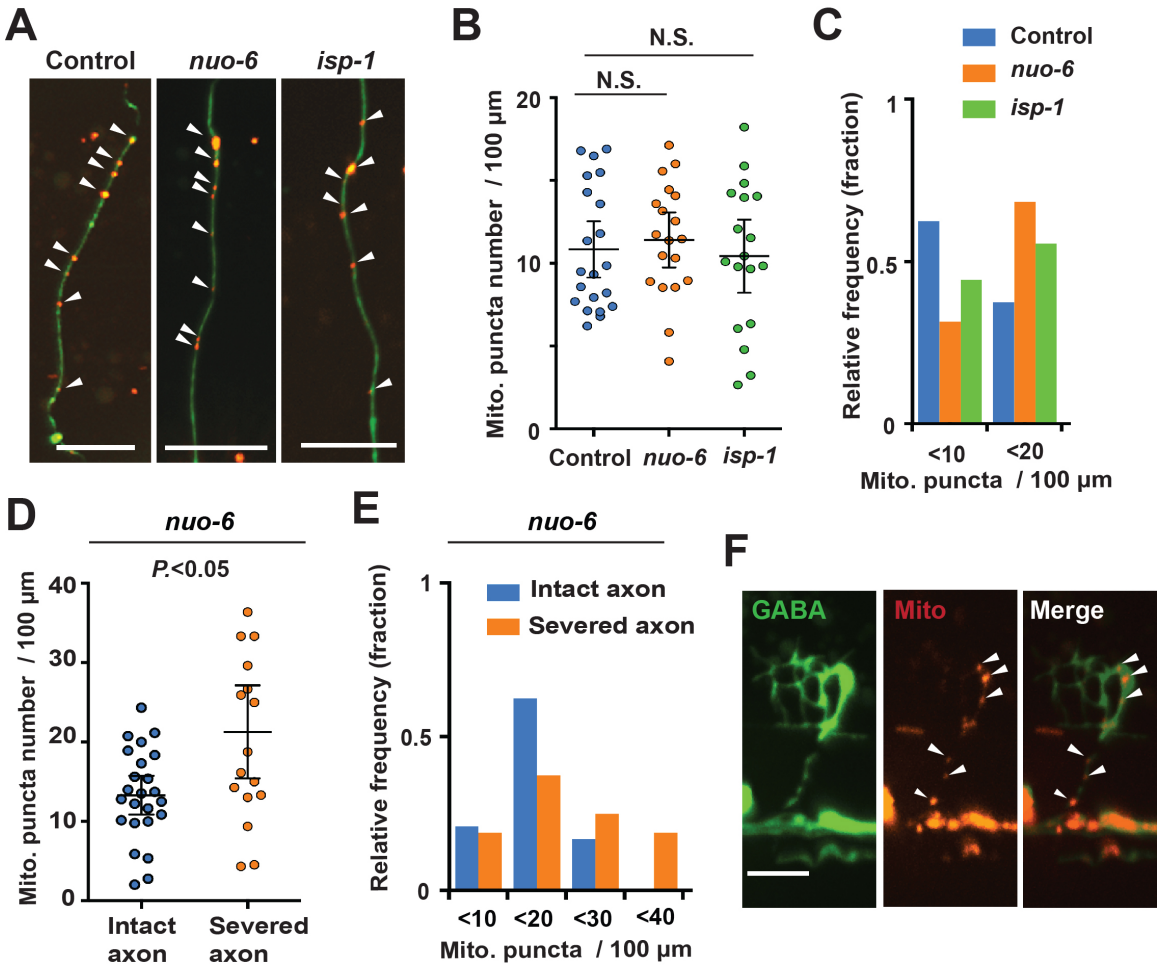

Figure S5. Related to Figure 6. Respiratory chain defective mutants have normal mitochondria density.

(A) Mitochondria in GABA axons of *nuo-6(qm200)* and *isp-1(qm150)* mutants. Scale bars are 20 µm.

(B and C) Scatter plot of mitochondria density (B) and binned frequency graph (C) in GABA axons of control, *nuo-6(qm200)* and *isp-1(qm150)* mutant animals 24 hours after axotomy. N.S. indicates not significant. Error bar indicate 95% confidence intervals. Statistical significance was calculated by the Mann–Whitney test.

(D and E) Scatter plot showing increased mitochondria density (D) and binned frequency graph (E) in GABA axons of *nuo-6(qm200)* at 24 hours after axotomy. Dots indicate individual axons. Error bars indicate 95% confidence interval. Statistical significance was calculated by the Mann–Whitney test.

(F) Mitochondria in GABA neurons of *nuo-6(qm200)* at 24 hours after axotomy Arrowheads indicate individual mCherry puncta. Scale bars are 5 µm.

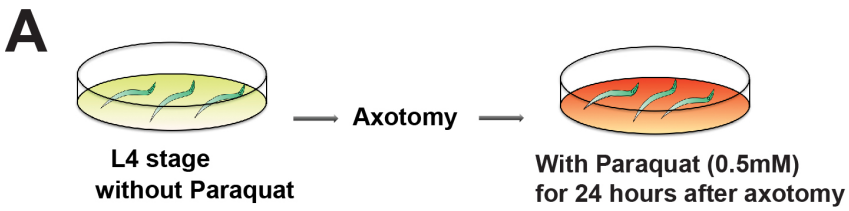
A
Axotomy
L4 stage
without Paraquat
With Paraquat (0.5mM)
for 24 hours after axotomy

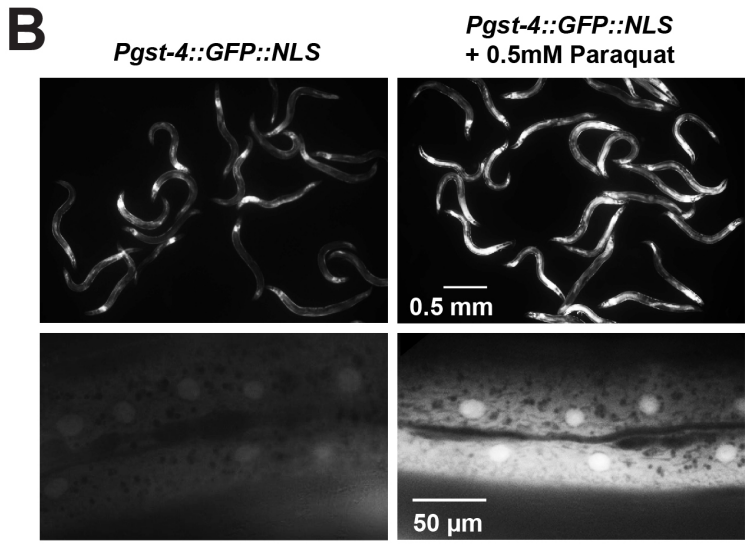
B
Pgst-4::GFP::NLS
Pgst-4::GFP::NLS
+ 0.5mM Paraquat
0.5 mm
50 µm

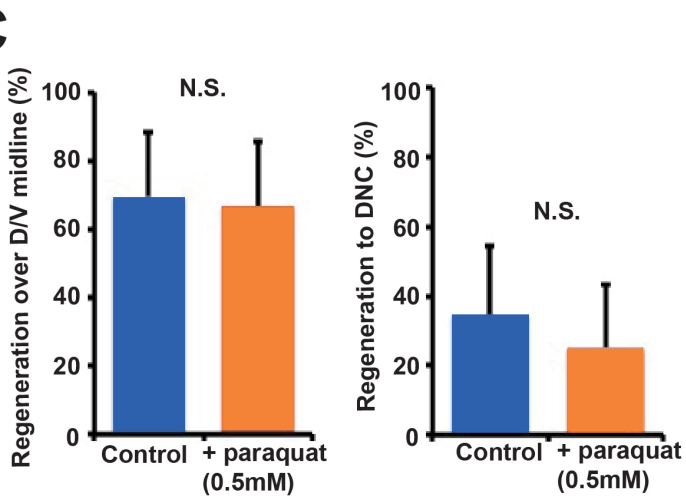
C
Regeneration over D/V midline (%)
N.S.
100
80
60
40
20
0
Control
+ paraquat
(0.5mM)
Regeneration to DNC (%)
N.S.
100
80
60
40
20
0
Control
+ paraquat
(0.5mM)

Figure S6. Related to Figure 6. Paraquat treatment does not reduce axon regeneration.

(A) Outline of the protocol to mildly increase ROS levels during axon regeneration. Paraquat (Ultra Scientific, U.S.A) assay was performed as described previously with slight modification (Lee et al., 2010; Runkel et al., 2013). Briefly, axotomized worms were placed on plates containing 0.5 mM paraquat and incubated for 24 hours at 20°C. After the incubation, axon regeneration was scored based on regrowth over dorsal-ventral midline or full regeneration to the dorsal nerve cord.

(B) The CL2166 reporter strain expressing GFP::NLS under the regulation of the *gst-4* promoter (Pgst-4::GFP::NLS) was used to determine whether paraquat (0.5mM) treatment induces oxidative stress. Animals incubated in 0.5 mM paraquat for 24 hours exhibit increased GFP expression compared to animals without paraquat treatment.

(C) Regeneration over dorsal-ventral midline (upper) and to the dorsal nerve cord (lower) of control and paraquat treated animals 24 hours after axotomy. N.S. indicates not significant. Error bars indicate 95% confidence interval. Statistical significance was calculated by Fisher's exact test. N = 23 (control) and 24 (paraquat treatment).

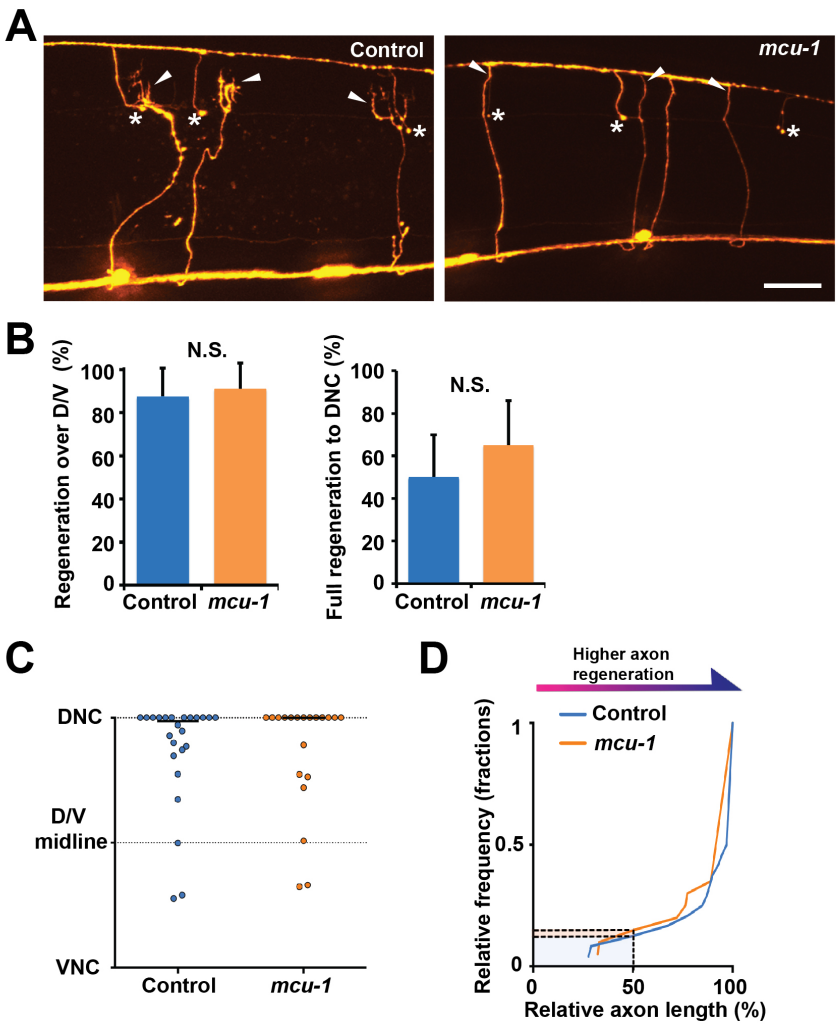

Figure S7. Related to Figure 6. Axon regeneration is normal in *mcu-1* mutants.

(A) GABA axons 24 hours after axotomy in control and *mcu-1(ju1154)* mutants. Scale bar is 20 μm.

(B) Regeneration over dorsal-ventral midline (left) and to the dorsal nerve cord (right) of controls and *mcu-1* mutant animals 24 hours after axotomy. Error bars indicate 95% confidence intervals. N.S. indicates not significant. N = 17 (control) and 23 (*mcu-1*).

(C) Scatter plot of relative axon length of GABA axons of controls and *mcu-1* mutant animals 24 hours after axotomy. Dots indicate individual axons and lines indicate median.

(D) Cumulative frequency histogram of relative axon lengths of GABA axons of controls and *mcu-1* mutant animals 24 hours after axotomy. Horizontal lines indicate the fraction of regenerated axons over dorsal-ventral midline.

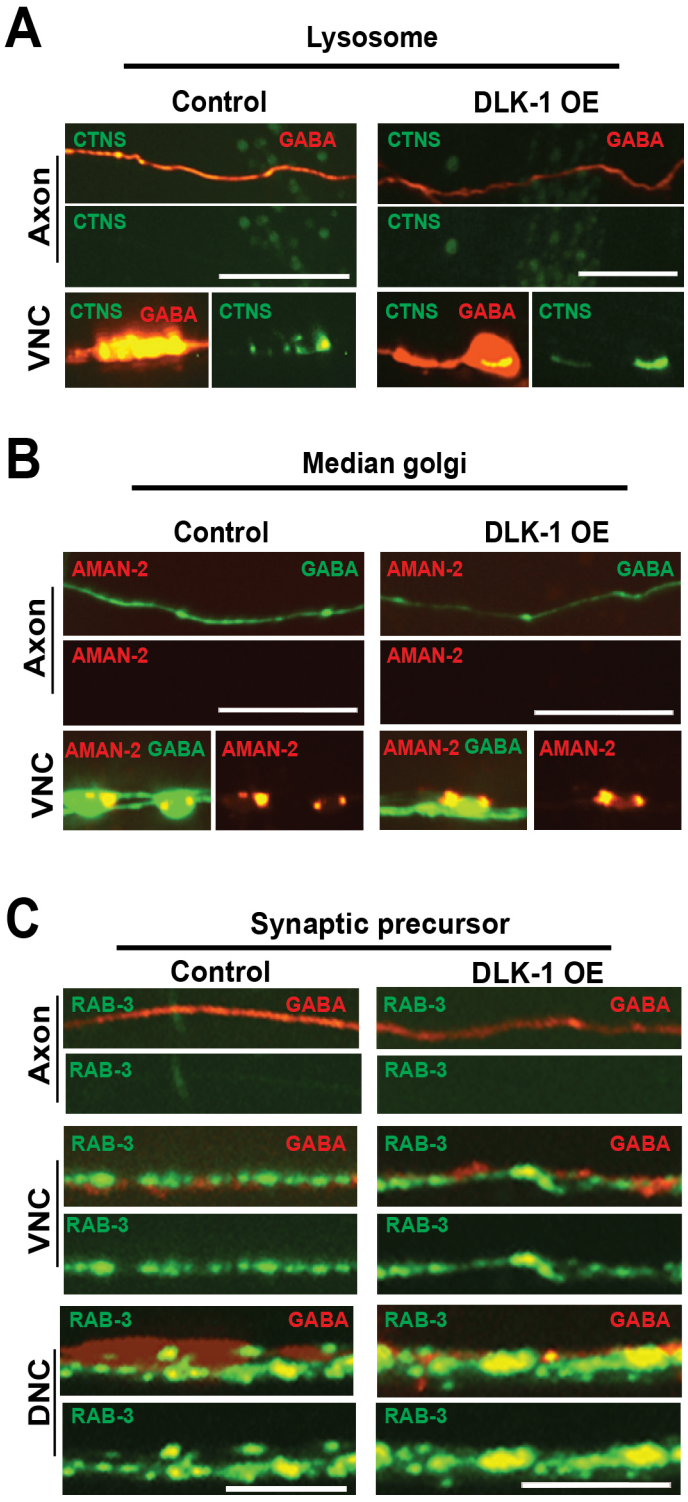
A
Lysosome
Control
DLK-1 OE
Axon
VNC
CTNS
GABA
B
Median golgi
AMAN-2
C
Synaptic precursor
RAB-3
DNC

Figure S8. Related to Figure 7. The effect of DLK-1 overexpression on positioning of intracellular organelles in GABA axons.

Localization of intracellular markers in GABA neurons. (A and B) Localization of lysosomes (A, marked by lysosomal cystine transporter, CTNS) and medial Golgi (B, marked by mannosidase II, AMAN-2). Each panel shows a representative micrograph of a cell body on the ventral nerve cord and of a commissural axon. In control and DLK-1 overexpression animals, these markers localize almost exclusively to perinuclear area in cell bodies. (C) Localization of synaptic vesicles and precursors (marked by RAB-3). In control and DLK-1 overexpression animals, this marker is localized to synaptic areas in the nerve cords, but is absent from commissural axons. Scale bars are 5 μm.

Table S1. Related to Figs. 1, 2, 4, 5, 7, and 8. Mitochondria density summary. Single GABA axons were severed and the number of mitochondrial puncta in the axons was scored and normalized by 100 um axon length. For P values, stars in the 'Genotype' column are provided to denote the genotype (within the group delimited by horizontal lines) against which the comparison was performed. Actual P values are provided in the 'P vs. control' column.

Genotype	Injury	Age when scored	Mitochondria density and 95% C.I.	# axon	P vs. control
oxIs12[Punc-47:GFP, lin-15+][*]	No	24 hr after L4	7.64±3.91	10	
oxIs12	Yes	24 hr after axotomy	22.89±4.57	14	<0.001[*]
oxIs12[**]	No	6 hr afterL4	8.55±1.75	24	
oxIs12	Yes	6 hr after axotomy	25.42±7.07	11	<0.001[**]
oxIs12[*]	No	24 hr after L4	8.97±1.59	22	
unc-70(s1502); oxIs12[**]	No	24 hr after L4	23.07±3.01	28	<0.001[*],
unc-22 RNAi	No	24 hr after L4	9.7±1.78	28	0.551[*], <0.001[**]
unc-70(s1502); oxIs12; unc-22 RNAi	No	24 hr after L4	11.64±2.32	27	0.088[*], <0.001[**]
oxIs12; Ex(Punc-47::mito::dendra2 + Pmyo-2::mCherry][*]	No	at L4 stage without photoconversion	0	18	
oxIs12; Ex(Punc-47::mito::dendra2 + Pmyo-2::mCherry]	Yes	at L4 stage without photoconversion	0.22±0.5	11	0.379[*]
oxIs12; Ex(Punc-47::mito::dendra2 + Pmyo-2::mCherry][**]	No	Immediately after photoconversion at L4 stage	0.08±0.18	26	
oxIs12; Ex(Punc-47::mito::dendra2 + Pmyo-2::mCherry]	Yes	Immediately after photoconversion at L4 stage	0.26±0.59	12	0.778[**],
oxIs12; Ex(Punc-47::mito::dendra2 + Pmyo-2::mCherry][***]	No	24 hr after L4 (after photoconversion)	3.38±0.96	14	<0.001[**]
oxIs12; Ex(Punc-47::mito::dendra2 + Pmyo-2::mCherry]	Yes	24 hr after L4 (after photoconversion)	5.57±1.53	19	<0.05[***]
oxIs12[*]	No	24 hr after L4	10.93±2.97	22	
pdr-1; oxIs12[**]	No	24 hr after L4	10.77±1.54	60	0.964[*]
pdr-1; oxIs12	Yes	24 hr after L4	16.84±4.56	23	<0.05[**]
juIs76[*]	No	24 hr after L4	9.7±3.1	25	
juIs76	Yes	24 hr after L4	17±2.39	42	<0.001[*]
aak-1; juIs76[**]	No	24 hr after L4	9.4±1.89	11	
aak-1; juIs76	Yes	24 hr after L4	15±4.55	18	<0.05[**], 0.306[*]
aak-2; juIs76[***]	No	24 hr after L4	8.3±2.23	17	
aak-2; juIs76	Yes	24 hr after L4	14±3.78	11	<0.05[***], 0.234[*]
oxIs12[*]	No	24 hr after L4	10.84±1.7	21	
isp-1(qm150); oxIs12	No	24 hr after L4	10.43±2.21	18	0.913[*]
nuo-6(qm200); oxIs12	No	24 hr after L4	11.4±1.65	19	0.449[*]
nuo-6(qm200); oxIs12[**]	No	24 hr after L4	13.30±2.44	24	
nuo-6(qm200); oxIs12	Yes	24 hr after L4	19.94±5.79	16	<0.05[**]
oxIs12[*]	No	24 hr after L4	11.49±1.83	53	
oxIs12[**]	Yes	24 hr after axotomy	22.34±2.6	80	<0.001[*]
dlk-1(ju476); oxIs12[***]	No	24 hr after L4	11.25±1.09	42	

dlk-1(ju476); oxIs12	Yes	24 hr after axotomy	18.37±2.95	43	<0.001[***], 0.027 [**]
oxIs12[*]	No	24 hr after L4	10.47±1.96	35	
oxIs12 ; wpIs9[Punc-47:DLK-1mini-GFP, ccGFP] [**]	No	24 hr after L4	25.62±2.49	63	<0.001 [*]
juIs76; cebp-1(tm2807) [***]	No	24 hr after L4	8.28±2.65	23	<0.001 [**], 0.053 [*]
juIs76; wpIs9; cebp-1(tm2807)	No	24 hr after L4	5.94±0.94	35	<0.001 [**], <0.001 [*], 0.755[***]
oxIs12	No	24 hr after L4	11.14±2.67	32	
oxIs12; [Punc-47:miro-1 OE]	No	24 hr after L4	15.14±1.48	68	<0.001
lin-15b(n744)X ; eri-1(mg366)IV ; rde-1(ne219)V: In[Punc-47p::rde-1::SL2::sid-1] ; control (RNAi)	No	24 hr after L4	6.88±0.64	69	
lin-15b(n744)X ; eri-1(mg366)IV ; rde-1(ne219)V: In[Punc-47p::rde-1::SL2::sid-1] ; miro-1 (RNAi)	No	24 hr after L4	4.41±0.76	31	<0.001
juIs76[*]	No	24 hr after L4	11±3.74	18	
miro-1; miro-2; juIs76[**]	No	24 hr after L4	4.1±1.96	23	<0.001[*]
miro-1; miro-2; wpIs7[Punc-47:DLK-1mini-GFP, ccGFP]; juIs76	Yes	24 hr after L4	7.7±1.35	39	<0.005[**],0.269[*]

Supplemental Experimental Procedures:

C. elegans.

C. elegans were fed OP50 and maintained on NGM plates at 20^{o}C. The transgenes *oxIs12[Punc-47::gfp]* (McIntire et al., 1997), *juIs76[Punc-25::gfp]* (Jin et al., 1999) and *wpIs40[Punc-47::mCherry]* mark the GABAergic nervous system. A complete list of all strains used in this study and their genotypes is in the supplementary procedures.

To make transgenic animals, the relevant constructs were microinjected into the worm distal gonad syncytium (Mello and Fire, 1995). The concentration of each injected plasmid was as followss: *Punc-47::tom-20::mCherry* (5 ng/µl), *Punc-47::mito::GFP* (5 ng/µl), *Punc-47::tom-20::Dendra2* (5 ng/µl), *Punc-47::drp-1::TagRFP* (15 ng/µl), *Punc-47:: GFP::CTNS* (5 ng/µl), *Punc-47::miro-1* (10 ng/µl), *Punc-25::aman-2::mCherry* (5 ng/µl). *Pmyo-2::mCherry marker* (2 ng/µl) was used as an injection marker. Transgenic worms were selected based on *Pmyo-2::mCherry* expression. The *Punc-25::aman-2::mCherry* was generously provided by Dr. Cori Bargmann.

Laser Axotomy and axon regeneration analysis.

Laser axotomy was performed as described previously (Byrne et al., 2011). Briefly, L4 stage animals were mounted on 2% agarose pad on glass slides and visualized with a Nikon Eclipse 80i microscope using a 100x Plan ApoVC lens (1.4 NA). The three axons among the seven most posterior VD/DD GABA motor neurons were cut using a Micropoint laser at 10 pulses, 20 Hz (Photonic Instruments). Animals were recovered to fresh NGM plates and analyzed for degree of axonal regeneration or mitochondria density 6, 12, or 24 hours after axotomy. Presence of the severed distal stump was used as evidence for successful surgery.

Full regrowth to the dorsal nerve cord or over the dorsal-ventral midline was scored and considered as a successful regeneration. To determine the relative axon length after nerve injury, the injured axon length was normalized by the distance between ventral and dorsal nerve cords 24 hours after axotomy.

Molecular Biology

Gateway recombination (Invitrogen) was used to generate *Punc-47::mito::GFP, Punc-47::GFP::ctns,* and *Punc-47::miro-1*. To create the entry clones, *ctns-1* and *miro-1* coding sequence were amplified from the *Punc-129::cnts-1::GFP* and a cDNA library using Phusion High-Fidelity DNA Polymerase (NEB) or Q5 High-Fidelity DNA polymerase (NEB). Amplified PCR fragments were cloned into pDONR 221 and subsequently used for LR reaction (Invitrogen). Gibson cloning was used to generate *Punc-47::mito::Dendra2.* The Dendra2 coding sequence was amplified from the engineered Dendra2 DNA plasmid, generously provided by Dr. David Sherwood. Amplified Dendra2 was cloned to generate a plasmid encoding *Punc-47* and *Dendra2.* PCR was used to amplify the entire sequence of the *Punc-47-Dendra2* plasmid, as well as the *tom-20* mitochondrial targeting sequence, and assembled in a Gibson reaction. *Punc-129::cnts-1::GFP* was generously provided by Dr. Colon-Ramos.

The primers used:

mito Fw tcacatttatttcattacagatggcactcctgcaatcacg
unc-47p Rv cgtgattgcaggagtgccatctgtaatgaaataaatgtg
ctns 221 FW ggggacaagtttgtacaaaaaagcaggctatatgctagcaaaaatgagtttcccgg
ctns 221 Rev ggggaccactttgtacaagaaagctgggtatctgatgccgcatagttaag
miro1 221 FW ggggacaagtttgtacaaaaaagcaggcttcatgagcgacgacgagacgttg
miro1 221 Rev ggggaccactttgtacaagaaagctgggttacagatttttcaagactaggaaac
dendra 1 FW gacaagtttgtacaaaaaagcaggctaaaaatgtcggaca
dendra 2 Rev tgtccgacatttttagcctgctttttgtacaaacttgtc
dendra 3 FW tccgcctccatgaaccttattaaggaagatatga
dendra 4 Rev ggttcatggaggcggatccggcggacaagaaagctgggtttcca

Feeding mediated RNA interference

RNAi was performed as described previously with minor modifications (Kamath et al., 2001). NGM plates with 25–50 µg/ml carbenicillin and 1 mM isopropyl β-D-1-thiogalactopyranoside were seeded with HT115 cells containing L4440 empty-vector control (pPD129.36) or plasmid targeting *miro-1* or *unc-22*. GABAergic specific RNAi was achieved using XE1375 *lin-15(n744) X ; eri-1(mg366) IV ; rde-1(ne219) V ; wpSi1[Punc-47::rde-1:SL2:sid-1, Cbunc-119(+)] II ; wpIs36[Punc-47::mCherry] I* (Firnhaber and Hammarlund, 2013). We also used *unc-22* (pLT61.1) for RNAi in the *unc-70(s1502)* background to prevent body bending and subsequent axon breakage. We placed L1 stage worms on RNAi plates and then examined L4- or young adult-stage animals from subsequent generations for testing mitochondria density in the *unc-70(s1502); unc-22(RNAi)* and regeneration phenotypes in other strains.

***C. elegans* strains**

Strain	Genotype	Annotation on the figure
XE1007	*oxIs12[Punc-47::GFP] X*	"Control" in most figures if there is no comment below
XE1828	*unc-70(s1502)/eT1[bli-4(e937) let-?(q782) qIs48] V; wpEx246[Punc-47::tom-20::mCherry + Punc-47::GFP::Pmyo-2::mCherry]*	"*unc-70* null" in figure 1H
XE1822	*oxIs12[Punc-47::GFP] X, wpEx246[Punc-47::mito::mCherry + Pmyo-2::mCherry]*	Figures 1B to 1G
XE1832	*drp-1(tm1108) IV; oxIs12[Punc-47::GFP] X*	*"drp-1* null" in figures 6B to 6F
XE1834	*wpIs40[Punc-47::mCherry]; wpEx270[Punc-47::mito::GFP + Pmyo-2::mCherry],*	"Control" in figure 6A
XE1833	*drp-1(tm1108) IV; wpIs40[Punc-47::mCherry]; wpEx270[Punc-47::mito::GFP + Pmyo-2::mCherry]*	*"drp-1* null" in figure 6A
XD1831	*drp-1(tm1108) IV; wpIs40[Punc-47::mCherry]; wpEx269[Punc-47::drp-1::tagRFP + Punc-47::mito::GFP +Pmyo-2::mCherry]*	*"drp-1* null + *Pgaba::*DRP-1 OE" in figure 6A
XE1830	*drp-1(tm1108) IV; oxIs12[Punc-47::GFP] X; wpEx271[Punc-47::drp-1::tagRFP + Pmyo-2::mCherry]*	*"GABA* + *Pgaba::*DRP-1 OE" in figures 6D and 6G
XE1375	*wpIs36[Punc-47::mCherry] I; wpSi1[Punc-47::rde-1:SL2:sid-1, Cbunc-119(+)] II; eri-1(mg366) IV; rde-1(ne219) V; lin-15B(n744) X;*	"Control" and as a background for "*miro-1* RNAi" in figures 4D to 4G
XE1844	*wpIs36[Punc-47::mCherry] I; wpSi1[Punc-47::rde-1:SL2:sid-1, Cbunc-119(+)] II; eri-1(mg366) IV; rde-1(ne219) V; lin-15B(n744) X;wpEx270[Punc-47::mito::GFP + Pmyo-2::mCherry]*	"Control" and as a background for "*miro-1* RNAi" in figures 4B and 4C
XE1845	*oxIs12[Punc-47::GFP] X, wpEx273[Punc-47::mito::mCherry + Pmyo-2::mCherry]*	"Control" in figures 5A and 5B
XE1846	*oxIs12[Punc-47::GFP] X, wpEx272[Punc-47::mito::mCherry + Punc-47::miro-1 + Pmyo-2::mCherry]*	*"miro-1* OE" in figures 5A, 5B, and 5C
XE1823	*oxIs12[Punc-47::GFP] X, wpEx268[Punc-47::mito::mCherry + Pmyo-2::mCherry]*	"Control" in figures S5A to S5F
XE1826	*isp-1 (qm150)IV;; oxIs12[Punc-47::GFP] X; wpEx268 [Punc-47::tom-20::mCherry + Pmyo-2::mCherry]*	*"isp-1"* in figures S5A to S5F
XE1827	*isp-1 (qm150)IV; oxIs12[Punc-47::GFP] X*	*"isp-1"* in figures 7A and 7B
XE1824	*nuo-6(qm200)I; oxIs12[Punc-47::GFP] X; wpEx268 [Punc-47::tom-20::mCherry + Pmyo-2::mCherry]*	*"nuo-6"* in figures S5A to S5F
XE1825	*nuo-6(qm200) I; oxIs12[Punc-47::GFP] X,*	*"nuo-6"* in figures 7A and 7B
XE1835	*oxIs12[Punc-47::GFP] X* ; *wpEx247[Punc-47::tom-20::mCherry + Pmyo-2::mCherry]*	"Control" in figures 8A to 8C
XE1836	*dlk-1 (ju476) I; oxIs12[Punc-47::GFP] X* ; *wpEx247[Punc-47::tom-20::mCherry + Pmyo-2::mCherry]*	*"dlk-1* null" in figures 8A to 8C
XE1829	*oxIs12[Punc-47::GFP] X* ; *wpEx248[Punc-47::tom-20::mCherry + Pmyo-2::mCherry]*	"Control" in figures 8D to 8E
XE1738	*wpIs9[Punc-47:DLK-1mini-GFP, ccGFP] II; oxIs12[Punc-47::GFP] X; wpEx248[Punc-47::tom-20::mCherry + Pmyo-2::mCherry]*	"DLK-1 OE" in figure 8
XE1739	*cebp-1(tm2807) X; juIs76[Punc-25::GFP] II*; *wpEx248[Punc-47::tom-20::mCherry + Pmyo-2::mCherry]*	*"cebp-1"* in figure 8

XE1740	*wpIs9[Punc-47:DLK-1mini-GFP, ccGFP] II; juIs76[Punc-25::GFP] II* ; *cebp-1(tm2807) X; wpEx248[Punc-47::tom-20::mCherry + Pmyo-2::mCherry]*	*"cebp-1* + DLK-1 OE" in figure 8
XE1837	*juIs76[Punc-25::GFP] II* ; *wpEx248[Punc-47::tom-20::mCherry + Pmyo-2::mCherry]*	Figures 3 and S4
XE1847	*mcu-1(ju1154) IV; wpIs40[Punc-47::mCherry]*	*"mcu-1"* in figure S7
XE1348	*wpIs40[Punc-47::mCherry] V*	"Control" in figure S7
XE1838	*jsIs682 III[Prab-**3**::gfp::rab-**3**; lin-15(+)] III; wpIs40[Punc-47::mCherry] V; lin-15B&lin-15A(n765) X*	"Control" in figure S8C
XE1339	*wpIs9[Punc-47:DLK-1mini-GFP, ccGFP] II; wpIs40[Punc-47::mCherry] V; jsIs682 III[Prab-**3**::gfp::rab-**3**; lin-15(+)]; lin-15B&lin-15A(n765) X*	"DLK-1 OE" in figure S8C
XE1840	*wpIs40[Punc-47::mCherry] V; wpEx274[Punc-47::GFP::CNTS + Pmyo-2::mCherry]*	"Control" in figure S8A
XE1841	*wpIs9[Punc-47:DLK-1mini-GFP, ccGFP] II; wpIs40[Punc-47::mCherry] V; wpEx274Punc-47::GFP::CNTS + Pmyo-2::mCherry]*	"DLK-1 OE" in figure S8A
XE1842	*oxIs12[Punc-47::GFP] X; wpEx275[Punc-25::aman-2::mCherry + Pmyo-2::mCherry]*	"Control" in figure S8B
XE1843	*wpIs9[Punc-47:DLK-1mini-GFP, ccGFP] II; oxIs12[Punc-47::GFP] X; wpEx275[Punc-25::aman-2::mCherry + Pmyo-2::mCherry]*	"DLK-1 OE" in figure S8B
XE1120	*juIs76[Punc-25::GFP] II*;	"Control" in figure S4A
XE1877	*juIs76[Punc-25::GFP] II*; *aak-1(tm1944) III*	"*aak-1*" in figure S4A
XE1878	*juIs76[Punc-25::GFP] II*; *aak-2(ok524) X*	"*aak-2*" in figure S4A
XE1879	*juIs76[Punc-25::GFP] II*; *wpEx248[Punc-47::tom-20::mCherry + Pmyo-2::mCherry]*	"Control" in figure S4C
XE1880	*juIs76[Punc-25::GFP] II*; *aak-1(tm1944) III; wpEx248[Punc-47::tom-20::mCherry + Pmyo-2::mCherry]*	"*aak-1*" in figure S4C
XE1881	*juIs76[Punc-25::GFP] II*; *aak-2(ok524) X; wpEx248[Punc-47::tom-20::mCherry + Pmyo-2::mCherry]*	"*aak-2*" in figure S4C
XE1882	*pdr-1(gk448) III; oxIs12[Punc-47::GFP] X; wpEx248[Punc-47::tom-20::mCherry + Pmyo-2::mCherry]*	"*pdr-1"* in figure S2
XE1883	*wpIs7[Punc-47:DLK-1mini-GFP, ccGFP] I; juIs76[Punc-25::GFP] II; miro-1(tm1966) IV; miro-2(tm2933)X;*	"*miro-1; miro-2*+DLK-1 OE" in figures 9A and 9B
XE1884	*wpIs7[Punc-47:DLK-1mini-GFP, ccGFP] I; juIs76[Punc-25::GFP] II;*	"DLK-1 OE" in figures 9A and 9B
XE1885	*juIs76[Punc-25::GFP] II; miro-1(tm1966) IV; miro-2(tm2933)X;*	"*miro-1; miro-2*" in figures 9A and 9B
XE1886	*wpIs7[Punc-47:DLK-1mini-GFP, ccGFP] I; juIs76[Punc-25::GFP] II; miro-1(tm1966) IV; miro-2(tm2933)X; wpEx248[Punc-47::tom-20::mCherry + Pmyo-2::mCherry]*	"*miro-1; miro-2*+DLK-1 OE" in figures 9D and 9E
XE1887	*wpIs7[Punc-47:DLK-1mini-GFP, ccGFP] I; juIs76[Punc-25::GFP] II; wpEx248[Punc-47::tom-20::mCherry + Pmyo-2::mCherry]*	*"DLK-1 OE"* in figures 9D and 9E

XE1888	*juIs76[Punc-25::GFP] II; miro-1(tm1966) IV; miro-2(tm2933)X; wpEx248[Punc-47::tom-20::mCherry + Pmyo-2::mCherry]*	"*miro-1; miro-2*" in figures 9D and 9E
XE1889	*juIs76[Punc-25::GFP] II; wpEx248[Punc-47::tom-20::Dendra2 + Pmyo-2::mCherry]*	in figures 2 and S1B
XE1890	*wpEx248[Punc-47::tom-20::Dendra2 + Pmyo-2::mCherry]*	in figure S1A

Supplemental References

Byrne, A.B., Edwards, T.J., and Hammarlund, M. (2011). In vivo laser axotomy in C. elegans. Journal of visualized experiments : JoVE.

Firnhaber, C., and Hammarlund, M. (2013). Neuron-specific feeding RNAi in C. elegans and its use in a screen for essential genes required for GABA neuron function. PLoS genetics *9*, e1003921.

Jin, Y., Jorgensen, E., Hartwieg, E., and Horvitz, H.R. (1999). The Caenorhabditis elegans gene unc-25 encodes glutamic acid decarboxylase and is required for synaptic transmission but not synaptic development. The Journal of neuroscience : the official journal of the Society for Neuroscience *19*, 539-548.

Kamath, R.S., Martinez-Campos, M., Zipperlen, P., Fraser, A.G., and Ahringer, J. (2001). Effectiveness of specific RNA-mediated interference through ingested double-stranded RNA in Caenorhabditis elegans. Genome biology *2*, RESEARCH0002.

Lee, S.J., Hwang, A.B., and Kenyon, C. (2010). Inhibition of respiration extends C. elegans life span via reactive oxygen species that increase HIF-1 activity. Current biology : CB *20*, 2131-2136.

McIntire, S.L., Reimer, R.J., Schuske, K., Edwards, R.H., and Jorgensen, E.M. (1997). Identification and characterization of the vesicular GABA transporter. Nature *389*, 870-876.

Mello, C., and Fire, A. (1995). DNA transformation. Methods in cell biology *48*, 451-482.
Runkel, E.D., Liu, S., Baumeister, R., and Schulze, E. (2013). Surveillance-activated defenses block the ROS-induced mitochondrial unfolded protein response. PLoS genetics *9*, e1003346.